

## ESTIMATION OF RELAXATION AND THERMALIZATION TIMES IN MICROSCALE HEAT TRANSFER MODEL

BOHDAN MOCHNACKI

*Częstochowa University of Technology, Częstochowa, Poland and  
Higher School of Labour Safety Management, Katowice, Poland  
e-mail: bohdan.mochnacki@im.pcz.pl*

MAREK PARUCH

*Silesian University of Technology, Institute of Computational Mechanics and Engineering, Gliwice, Poland  
e-mail: marek.paruch@polsl.pl*

The energy equation corresponding to the dual phase lag model (DPLM) results from the generalized form of the Fourier law, in which the two ‘delay times’ (relaxation and thermalization time) are introduced. The DPLM should be used in the case of microscale heat transfer analysis, in particular when thermal processes are characterized by extremely short duration (e.g. ultrafast laser pulse), considerable temperature gradients and very small dimensions (e.g. thin metal film). In this paper, the problem of relaxation and thermalization time identification is discussed, at the same time the heat transfer processes proceeding in the domain of a thin metal film subjected to a laser beam are analyzed. The solution presented bases on the application of evolutionary algorithms. The additional information concerning the transient temperature distribution on a metal film surface is assumed to be known. At the stage of numerical realization, the finite difference method (FDM) is used. In the final part of the paper, an example of computations is presented.

*Key words:* microscale heat transfer, laser heating, dual phase lag model, inverse problem

### 1. Governing equations

The following form of the generalized Fourier law is considered

$$\mathbf{q}(x, t + \tau_q) = -\lambda \nabla T(x, t + \tau_T) \quad (1.1)$$

where  $\mathbf{q}$  is the unitary heat flux,  $\lambda$  is the thermal conductivity,  $\nabla T$  is the temperature gradient,  $\tau_q$  is the relaxation time (the mean time for electrons to change their energy states),  $\tau_T$  is the thermalization time (the mean time required for electrons and lattice to reach equilibrium).

The DPL equation results from considerations concerning the parabolic two-temperature model (Al-Nimr, 1997; Chen and Beraun, 2001; Majchrzak and Poteralska, 2011; Majchrzak *et al.*, 2009), in particular the energy equations determining the heat transfer in the electron gas and the metal lattice are taken into account. In the case of pure metals, the two-temperature model takes the form

$$c_e(T_e) \frac{\partial T_e}{\partial t} = \nabla[\lambda_e(T_e) \nabla T_e] - G(T_e - T_l) \quad c_l(T_l) \frac{\partial T_l}{\partial t} = G(T_e - T_l) \quad (1.2)$$

where  $T_e = T_e(x, t)$ ,  $T_l = T_l(x, t)$  are the temperatures of electrons and lattice,  $c_e(T_e)$ ,  $c_l(T_l)$  are the volumetric specific heats (thermal capacities),  $\lambda_e(T_e)$ ,  $\lambda_l(T_l)$  are the thermal conductivities,  $G$  is the coupling factor – this parameter characterizes the energy exchange between a phonon and electrons (Lin and Zhigilei, 2008).

In Fig. 1 (see Majchrzak and Poteralska, 2011) an example of numerical solution obtained using the two temperature parabolic model is shown. The metal film (Ti) subjected to a laser pulse has been considered and the heating (cooling) curves correspond to the film surface. Differences between  $T_e$  and  $T_l$  are visible, the time of both temperatures equalization corresponds to the thermalization one.

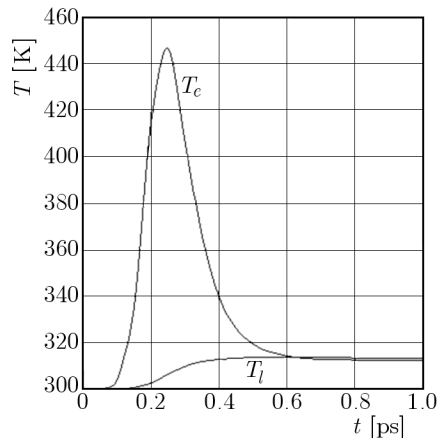


Fig. 1. Changes of surface temperatures

Using a certain elimination technique, equations (1.2) can be substituted by a single equation containing the second derivative of temperature with respect to time and a higher-order mixed derivative in both time and space. Let us assume that the volumetric specific heats  $c_e$  and  $c_l$  are constant values (this simplification is acceptable when the changes of temperature during the heating process are not very big). So, from equation (1.2)<sub>1</sub> it results that

$$T_e = T_l + \frac{c_l}{G} \frac{\partial T_l}{\partial t} \quad (1.3)$$

Putting (1.2)<sub>2</sub> into (1.1), one has

$$c_e \left( \frac{\partial T_l}{\partial t} + \frac{c_l}{G} \frac{\partial^2 T_l}{\partial t^2} \right) = \nabla(\lambda_e \nabla T_l) + \frac{c_l}{G} \nabla \left[ \lambda_e \frac{\partial}{\partial t} (\nabla T_l) \right] - c_l \frac{\partial T_l}{\partial t} \quad (1.4)$$

this means

$$(c_e + c_l) \left[ \frac{\partial T_l}{\partial t} + \frac{c_e}{c_l} G (c_e + c_l) \frac{\partial^2 T_l}{\partial t^2} \right] = \nabla(\lambda_e \nabla T_l) + \frac{c_l}{G} \frac{\partial}{\partial t} [\nabla \lambda_e (\nabla T_l)] \quad (1.5)$$

Denoting

$$\tau_T = \frac{c_l}{G} \quad \tau_q = \frac{1}{G} \left( \frac{1}{c_e} + \frac{1}{c_l} \right)^{-1} \quad (1.6)$$

finally one obtains

$$c \left[ \frac{\partial T(x, t)}{\partial t} + \tau_q \frac{\partial^2 T(x, t)}{\partial t^2} \right] = \nabla[\lambda \nabla T(x, t)] + \tau_T \nabla \left[ \lambda \frac{\partial \nabla T(x, t)}{\partial t} \right] \quad (1.7)$$

where  $T(x, t) = T_l(x, t)$  is the macroscopic lattice temperature (Ozisik and Tzou, 1994),  $c = c_l + c_e$  is the effective volumetric specific heat resulting from the serial assembly of electrons and phonons and  $\lambda = \lambda_e$  (Ozisik and Tzou, 1994).

Another approach to the DPLM formulation is also possible and the following mathematical considerations were presented in Majchrzak *et al.* (2009).

Using the Taylor series expansions, the following first-order approximation of equation (1.1) can be taken into account

$$\mathbf{q}(x, t) + \tau_q \frac{\partial \mathbf{q}(x, t)}{\partial t} = -\lambda \left[ \nabla T(x, t) + \tau_T \frac{\partial \nabla T(x, t)}{\partial t} \right] \quad (1.8)$$

or

$$-\mathbf{q}(x, t) = \tau_q \frac{\partial \mathbf{q}(x, t)}{\partial t} + \lambda \nabla T(x, t) + \tau_T \lambda \frac{\partial \nabla T(x, t)}{\partial t} \quad (1.9)$$

This formula should be introduced to the well known macroscopic energy equation

$$c \frac{\partial T(x, t)}{\partial t} = -\nabla \cdot \mathbf{q}(x, t) \quad (1.10)$$

This means

$$c \frac{\partial T(x, t)}{\partial t} = \tau_q \frac{\partial}{\partial t} [\nabla \mathbf{q}(x, t)] + \nabla [\lambda \nabla T(x, t)] + \tau_T \nabla \left[ \lambda \frac{\partial \nabla T(x, t)}{\partial t} \right] \quad (1.11)$$

Substituting  $-\nabla \mathbf{q}$  by  $c(T) \partial T / \partial t$ , one obtains the same equation as equation (1.7)

$$c \left[ \frac{\partial T(x, t)}{\partial t} + \tau_q \frac{\partial^2 T(x, t)}{\partial t^2} \right] = \nabla [\lambda \nabla T(x, t)] + \tau_T \nabla \left[ \lambda \frac{\partial \nabla T(x, t)}{\partial t} \right] \quad (1.12)$$

In this paper, the problem of heat diffusion in the presence of volumetric internal heat sources  $Q(x, t)$  is considered. It can be shown that in this case, equation (1.12) must be supplemented by additional components, in particular

$$\begin{aligned} c \left[ \frac{\partial T(x, t)}{\partial t} + \tau_q \frac{\partial^2 T(x, t)}{\partial t^2} \right] &= \nabla [\lambda \nabla T(x, t)] + \tau_T \nabla \left[ \lambda \frac{\partial \nabla T(x, t)}{\partial t} \right] \\ &+ Q(x, t) + \tau_q \frac{\partial Q(x, t)}{\partial t} \end{aligned} \quad (1.13)$$

It results from the fact that the thermal interactions between external heating (laser pulse) and the domain of the metal film are taken into account by the introduction of an additional term supplementing the DPLM, in particular a function corresponding to the volumetric internal heat sources  $Q(x, t)$  is considered. This approach is often used (e.g. Al-Nimr, 1997). The formula determining the capacity of the internal heat sources takes a form (1D problem – Chen and Beraun (2001), Chen *et al.* (2004))

$$Q(x, t) = \sqrt{\frac{\mu}{\pi}} \frac{1-R}{t_p \delta} I_0 \exp \left[ -\frac{x}{\delta} - \mu \left( \frac{t-2t_p}{t_p} \right)^2 \right] \quad (1.14)$$

where  $I_0$  is the laser intensity which is defined as the total energy carried by a laser pulse per unit cross-section of the laser beam,  $t_p$  is the characteristic time of the laser pulse,  $\delta$  is the characteristic transparent length of irradiated photons called the absorption depth,  $R$  is the surface reflectivity,  $\mu = 4 \ln 2$ . The local and temporary value of  $Q$  results from the distance  $x$  between the surface subjected to laser action and the point considered. Using this approach, the no-flux boundary conditions for  $x = 0$  and  $x = L$  should be assumed.

In Fig. 2 the domain considered is shown and its geometrical features allows one to treat the problem as a 1D one.

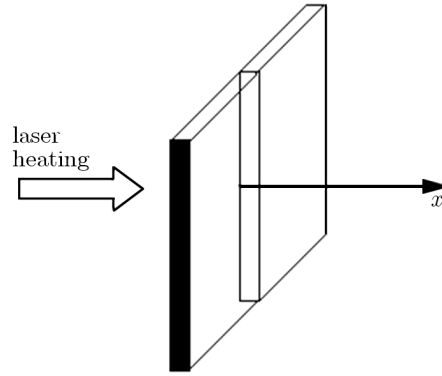


Fig. 2. Domain considered

**2. Numerical solution basing on fdm (a direct problem)**

At the stage of numerical modeling, the finite difference method has been used. The version proposed constitutes a generalization of the FDM variant proposed by Mochnacki and Suchy (1995). So, the following energy equation is considered

$$c \left[ \frac{\partial T(x, t)}{\partial t} + \tau_q \frac{\partial^2 T(x, t)}{\partial t^2} \right] = \frac{\partial}{\partial x} \left[ \lambda \frac{\partial T(x, t)}{\partial x} \right] + \tau_T \frac{\partial}{\partial t} \frac{\partial}{\partial x} \left[ \lambda \frac{\partial T(x, t)}{\partial x} \right] + Q(x, t) + \tau_q \frac{\partial Q(x, t)}{\partial t} \tag{2.1}$$

The differential mesh is created as a Cartesian product of spatial  $\Delta h$  and time  $\Delta t$  meshes. The time grid is defined as follows

$$\Delta t: t^0 < t^1 < \dots < t^{f-2} < t^{f-1} < t^f < \dots < t^F < \infty \tag{2.2}$$

while the spatial mesh is shown in Fig. 3.

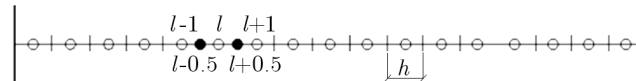


Fig. 3. The mesh

It is visible that the 'boundary' nodes are located at the distance  $0.5h$  from real boundaries (this type of discretization assures a very simple and exact approximation of boundary conditions, Mochnacki and Suchy (1995)).

The FDM approximation of the spatial differential operator can be taken in the form

$$\frac{\partial}{\partial x} \left( \lambda \frac{\partial T}{\partial x} \right)_i^f = \frac{T_{i+1}^f - T_i^f}{R_{i+1}^{f-1}} \Psi_{i+1} + \frac{T_{i-1}^f - T_i^f}{R_{i-1}^{f-1}} \Psi_{i-1} \tag{2.3}$$

where  $\Psi_{i+1} = \Psi_{i-1} = 1/h$  are the mesh shape functions, while

$$R_{i+1}^{f-1} = \frac{h}{2\lambda_i^{f-1}} + \frac{h}{2\lambda_{i+1}^{f-1}} \quad R_{i-1}^{f-1} = \frac{h}{2\lambda_i^{f-1}} + \frac{h}{2\lambda_{i-1}^{f-1}} \tag{2.4}$$

are the thermal resistances between the node  $i$  and adjoining the nodes  $i + 1, i - 1$ . The index  $f$  in formula (2.3) shows that the implicit differential scheme will be used here, at the same time,

the thermal conductivities are taken for the time  $t^{f-1}$  to obtain the linear form of final FDM equations. The FDM approximation of equation (2.1) for transition  $t^{f-1} \rightarrow t^f$  is of the form

$$\begin{aligned}
 c \frac{T_i^f - T_i^{f-1}}{\Delta t} + c\tau_q \frac{T_i^f - 2T_i^{f-1} + T_i^{f-2}}{(\Delta t)^2} &= \frac{T_{i+1}^f - T_i^f}{R_{i+1}^{f-1}} \Psi_{i+1} + \frac{T_{i-1}^f - T_i^f}{R_{i-1}^{f-1}} \Psi_{i-1} \\
 + \frac{\tau_T}{\Delta t} \left( \frac{T_{i+1}^f - T_i^f}{R_{i+1}^{f-1}} \Psi_{i+1} + \frac{T_{i-1}^f - T_i^f}{R_{i-1}^{f-1}} \Psi_{i-1} \right) & \\
 - \frac{\tau_T}{\Delta t} \left( \frac{T_{i+1}^{f-1} - T_i^{f-1}}{R_{i+1}^{f-1}} \Psi_{i+1} + \frac{T_{i-1}^{f-1} - T_i^{f-1}}{R_{i-1}^{f-1}} \Psi_{i-1} \right) + Q_i^f + \tau_q \left( \frac{\partial Q}{\partial t} \right)_i^f &
 \end{aligned} \tag{2.5}$$

and the last formula can be written as follows ( $i = 1, 2, \dots, N$ )

$$\begin{aligned}
 A_i T_{i-1}^f + B_i T_i^f + C_i T_{i+1}^f &= D_i T_{i-1}^{f-1} + E_i T_i^{f-1} + F_i T_{i+1}^{f-1} + \frac{\tau_q}{(\Delta t)^2} T_i^{f-2} \\
 - \frac{Q_i^f}{c} - \frac{\tau_q}{c} \left( \frac{\partial Q}{\partial t} \right)_i^f &
 \end{aligned} \tag{2.6}$$

where

$$\begin{aligned}
 A_i &= \frac{\Psi_{i-1}}{cR_{i-1}^{f-1}} \left( 1 + \frac{\tau_T}{\Delta t} \right) & C_i &= \frac{\Psi_{i+1}}{cR_{i+1}^{f-1}} \left( 1 + \frac{\tau_T}{\Delta t} \right) \\
 B_i &= -\frac{1}{\Delta t} \left( 1 + \frac{\tau_q}{\Delta t} \right) - A_i - C_i & D_i &= \frac{\Psi_{i-1}}{cR_{i-1}^{f-1}} \frac{\tau_T}{\Delta t} \\
 F_i &= \frac{\Psi_{i+1}}{cR_{i+1}^{f-1}} \frac{\tau_T}{\Delta t} & E_i &= -\frac{1}{\Delta t} \left( 1 + \frac{2\tau_q}{\Delta t} \right) - D_i - F_i
 \end{aligned} \tag{2.7}$$

Finally

$$A_i T_{i-1}^f + B_i T_i^f + C_i T_{i+1}^f = G_i^f \tag{2.8}$$

where

$$G_i^f = D_i T_{i-1}^{f-1} + E_i T_i^{f-1} + F_i T_{i+1}^{f-1} + \frac{\tau_q}{(\Delta t)^2} T_i^{f-2} - \frac{Q_i^f}{c} - \frac{\tau_q}{c} \left( \frac{\partial Q}{\partial t} \right)_i^f \tag{2.9}$$

The same equations are accepted for the nodes close to boundaries. It is enough to assume that the thermal resistances in the directions 'to boundary' are sufficiently big (e.g.  $10^{10}$ ), and then the non-flux condition is taken into account. The starting point of the numerical simulation process results from the initial conditions, in particular  $T_i^0 = T_i^1 = T_0$ ,  $i = 1, 2, \dots, N$ . The system of FDM equations (2.6) has been solved using the very effective Thomas algorithm for a three-diagonal linear system of algebraic equations (e.g. Mochnacki and Suchy, 1995).

### 3. Inverse problem

To solve the inverse problem, the least squares criterion is applied

$$S(\tau_q, \tau_T) = \frac{1}{MF} \sum_{i=1}^M \sum_{f=1}^F (T_i^f - T_{di}^f)^2 \tag{3.1}$$

where  $T_{di}^f$  and  $T_i^f = T(x_i, t^f)$  are the measured and estimated temperatures, respectively,  $M$  is the number of sensors (e.g. Majchrzak *et al.*, 2008; Mochnacki and Majchrzak, 2007). The minimum of functional (3.1) has been found using the evolutionary algorithms. So the direct problems have been solved and the results allow one to determine the time dependent surface temperature ( $x = 0$ ). Because the temperature history resulting from the numerical solution for the basic input data is very close to the experimental ones quoted in Chen and Beraun (2001), Tang and Araki (1999), Fig. 4, therefore this undisturbed numerical solution is assumed to be the base for the identification problem solution ('measured surface temperature'). So, the laser parameters determining capacity of the internal source function  $Q(x, t)$  and also the thermal conductivity and volumetric specific heat of gold are known, the parameters  $\tau_q$ ,  $\tau_T$  should be determined (from the practical standpoint, the experimental estimation of  $\tau_q$ ,  $\tau_T$  is not easy).

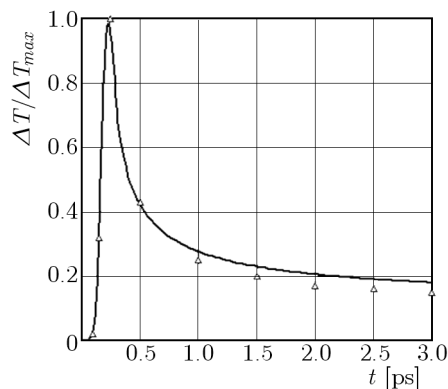


Fig. 4. Comparison with experimental data (Chen and Beraun, 2001)

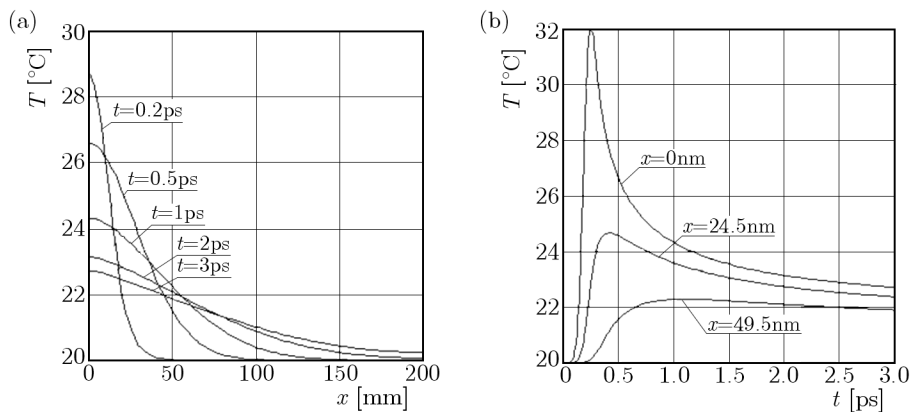


Fig. 5. (a) Temperature profiles, (b) cooling (heating) curves

In Figs. 5a and 5b, an example of the direct problem solution is shown. The layer is subjected to a short-pulse laser irradiation whose parameters are  $R = 0.93$  (reflectivity),  $I_0 = 13.7 \text{ J/m}^2$  (intensity),  $t_p = 0.1 \text{ ps} = 10^{-13} \text{ s}$  (time of laser pulse),  $\delta = 15.3 \text{ nm}$  (absorption depth). The following parameters of the gold thin film are assumed: thermal conductivity  $\lambda = 317 \text{ W/(mK)}$ , volumetric specific heat  $c = 2.4897 \text{ MJ/(m}^3\text{K)}$ , relaxation time  $\tau_q = 8.5 \text{ ps}$ , thermalization time  $\tau_T = 90 \text{ ps}$ . The initial temperature equals  $T_0 = 20^\circ\text{C}$  (see: Majchrzak *et al.*, 2009; Majchrzak and Poteralska, 2010).

Using the algorithm presented in the previous Section on the assumption that  $N = 200$  and  $\Delta t = 0.005 \text{ ps}$  the transient temperature field has been found. In Fig. 5a, the temperature profiles are shown, while Figs. 4 and 5b illustrate the courses of heating (cooling) curves at the points selected from the domain considered.

The identification of ‘delay’ times has been done using the evolutionary algorithms. In Table 1, the algorithm parameters are collected. The results obtained are presented in Table 2, and they are quite satisfactory.

**Table 1.** Evolutionary algorithm parameters

Number of generations	Number of chromosomes	Prob. of uniform mutation	Prob. of nonuniform mutation	Prob. of arithmetic crossover	Prob. of cloning
100	75	20%	30%	50%	10%

**Table 2.** Result of computations using the EA

Design variable	Exact value	Found value	Error [%]
$\tau_q$	$8.5 \cdot 10^{-12}$	$8.499999 \cdot 10^{-12}$	0
$\tau_T$	$90 \cdot 10^{-12}$	$89.99999 \cdot 10^{-12}$	0

Figures 6-9 show the process of identification using the evolutionary algorithm after 1st, 10th, 50th and 100th generations. The mark  $\times$  shows the position of the real value.

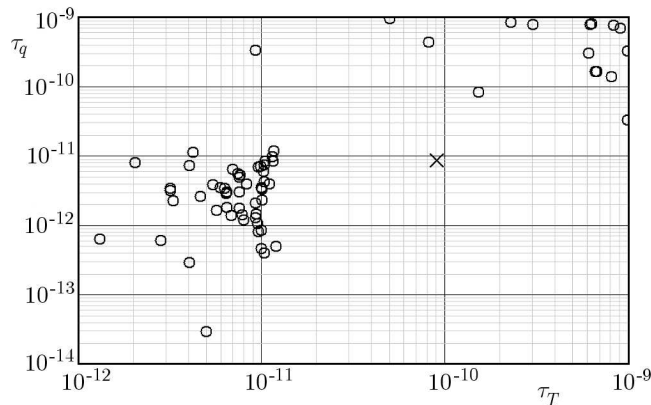


Fig. 6. The process of identification – evolutionary algorithm – after 1st generation

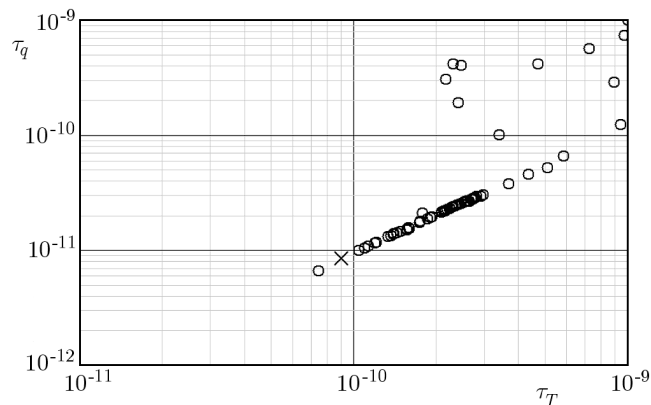


Fig. 7. The process of identification – evolutionary algorithm – after 10th generations

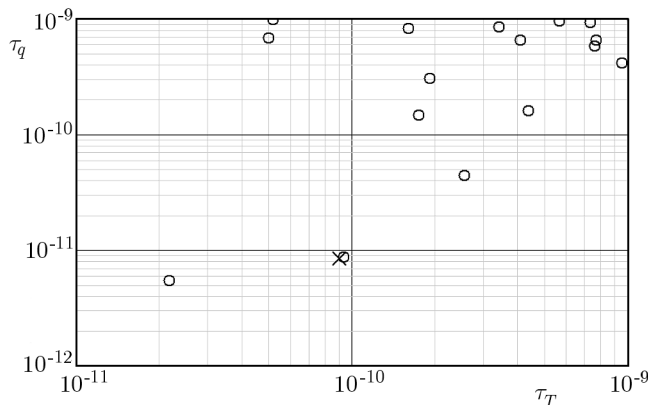


Fig. 8. The process of identification – evolutionary algorithm – after 50th generations

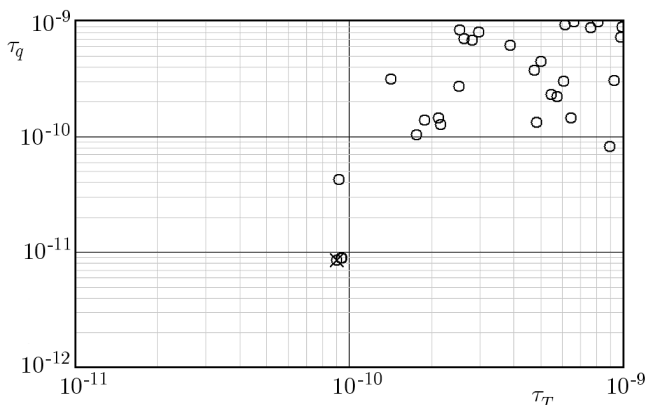


Fig. 9. The process of identification – evolutionary algorithm – after 100th generations

#### 4. Final remarks

The application of evolutionary algorithms for solutions of the identification problems is (from the numerical point of view) time-consuming. On the other hand, however, the mathematical and numerical problems connected with adequate algorithm construction seems to be essentially simpler in comparison with the very popular gradient methods. The exactness of estimation parameters  $\tau_q$ ,  $\tau_T$  is very good, and even in the case of real experimental data application the quality of the obtained results is also satisfactory. The details concerning the methods of indirect measurements of surface temperatures in the case of microscale domains can be found in Tang and Araki (1999). The future works will be connected with the problems concerning the micro models of crystallization (e.g. Lelito *et al.*, 2012).

#### *Acknowledgements*

This work has been supported by project No. 2012/05/B/ST8/01477 sponsored by the Polish National Science Centre for Research and Development.

#### References

1. AL-NIMR M.A., 1997, Heat transfer mechanisms during short duration laser heating of thin metal films, *International Journal of Thermophysics*, **18**, 5, 1257-1268
2. CHEN J.K., BERAUN J.E., 2001, Numerical study of ultrashort laser pulse interactions with metal films, *Numerical Heat Transfer, Part A*, **40**, 1-20

3. CHEN G., BORCA-TASCIUC D., YANG R.G., 2004, Nanoscale heat transfer, *Encyclopedia of Nanoscience and Nanotechnology*, **X**, 1-30
4. LELITO J., ŻAK P.L., GREER A.L., SUCHY J.S., KRAJEWSKI W.K., GRACZ B., SZUCKI M., SHIRZADI A.A., 2012, Crystallization model of magnesium primary phase in the AZ91/SiC composite, *Composites Part B: Engineering*, **43**, 8, 3306-3309
5. LIN Z., ZHIGILEI L.V., 2008, Electron-phonon coupling and electron heat capacity of metals under conditions of strong electron-phonon nonequilibrium, *Physical Review B*, **77**, 075133-1-075133-17
6. MAJCHRZAK E., MOCHNACKI B., GREER A.L., SUCHY J.S., 2009, Numerical modeling of short pulse laser interactions with multi-layered thin metal films, *CMES: Computer Modeling in Engineering and Sciences*, **41**, 2, 131-146
7. MAJCHRZAK E., MOCHNACKI B., SUCHY J.S., 2008, Identification of substitute thermal capacity of solidifying alloy, *Journal of Theoretical and Applied Mechanics*, **46**, 2, 257-268
8. MAJCHRZAK E., POTERALSKA J., 2010, Two-temperature microscale heat transfer model. Part 1: Determination of electrons parameters, *Scientific Research of the Institute of Mathematics and Computer Science*, Częstochowa, **9**, 1, 99-108
9. MAJCHRZAK E., POTERALSKA J., 2011, Two temperature model of microscopic heat transfer, *Computer Methods in Material Science*, **11**, 2, 337-342
10. MOCHNACKI B., MAJCHRZAK E., 2007, Identification of macro and micro parameters in solidification model, *Bulletin of the Polish Academy of Sciences – Technical Sciences*, **55**, 1, 107-113
11. MOCHNACKI B., SUCHY J.S., 1995, *Numerical Methods in Computations of Foundry Processes*, Polish Foundrymen's Technical Association, Cracow
12. OZISIK M.N., TZOU D.Y., 1994, On the wave theory in heat conduction, *Journal of Heat Transfer*, **116**, 526-535
13. TANG D.W., ARAKI N., 1999, Wavy, wavelike, diffusive thermal responses of finite rigid slabs to high-speed heating of laser-pulses, *International Journal of Heat and Mass Transfer*, **42**, 855-860

*Manuscript received November 27, 2012; accepted for print January 24, 2013*